Aging characteristics of nickel contact on p-type silicon

P. Chattopadhyay

Citation: Journal of Applied Physics **94**, 7149 (2003); doi: 10.1063/1.1591072
View online: http://dx.doi.org/10.1063/1.1591072
View Table of Contents: http://scitation.aip.org/content/aip/journal/jap/94/11?ver=pdfcov
Published by the AIP Publishing

Aging characteristics of nickel contact on *p*-type silicon

P. Chattopadhyay[a)]
Department of Electronic Science, University of Calcutta, 92, Acharyya Prafulla Chandra Road, Calcutta 700 009, India

(Received 22 November 2002; accepted 21 May 2003)

The effect of aging on the electrical properties of a Ni–*p*-Si contact was studied by measuring the electrical characteristics at different intervals of time. The current–voltage characteristics measured show a decrease in the current over time for the first few measurements at different aging times followed by an insignificant change for longer aging. The barrier height extracted from $I-V$ characteristics was found to increase from an initial value to a final higher value after a prolonged period of aging. This is the opposite of those normally exhibited by an aging $Al-SiO_2-p$-Si system [H. C. Card, IEEE Trans. Electron Devices **ED-23**, 538 (1976)]. Similar to the case of current, the device conductance and capacitance were also found to decrease with the aging time until they become saturated after longer periods of aging. The features of aging are explained by a theoretical model which considers the existence of an interfacial SiO_2 layer and Si traps in the interfacial region. It is shown that the concentration of silicon traps decays exponentially over time. The interpretation of the aging characteristics of a *Ni–p*-Si contact on the basis of exponential decay in the silicon trap concentration is in contrast to an $Al-SiO_2-p$-Si system where the aging behavior was accounted for in terms of the net growth in silicon concentration over time followed by saturation after longer aging. Analyses of the low and high frequency capacitance reveal two types of interface state that have different time constants and density. The time constants of these states were found to be dependent on the aging time via surface potential at the contact. © *2003 American Institute of Physics.* [DOI: 10.1063/1.1591072]

I. INTRODUCTION

The study of the aging properties of metal–semiconductor contacts is not only important to understanding the durability of such contacts for long term device application but also to realize the intricate interface phenomenon that relates interface states and interfacial contamination. Turner and Rhoderick[1] noticed considerable variation of the barrier height of a gold contact on a chemically prepared surface of silicon with aging. The effect of aging in an $Al-SiO_2-Si$ system was systematically examined by Card.[2] In the case of *p*-type devices, the barrier height was found to decrease with the aging time until a stable value is reached. The effect of aging in the case of *n*-type devices was found to be opposite. Interface contamination that leads to a reduction of mechanical strength was pointed out by Varma *et al.*[3] while studying gold and silver contacts on clean, oxidized silicon surfaces of silicon. Mottram *et al.*[4] observed aging of gold and copper contacts on silicon and found enhancement of the barrier height in copper contacts. The consistent observations of changing electrical characteristics of aging metal–semiconductor contacts have led to several concerns, such as the migration of charged ions and the possibility of interface reaction between the metal and the adjacent oxide.[5]

The role of the oxide is particularly important for devices fabricated on chemically prepared surfaces or devices in which an oxide layer has been deliberately introduced. In the case of an $Al-SiO_2-Si$ system, silicon atoms liberated by the reaction of aluminum with an adjacent SiO_2 layer are the main source of systematic variation of the barrier height with the aging time.[6] Being tetravalent in character, these free silicon atoms act as fourfold electron traps. The trapping of electrons at these free silicon atoms yields negative charge density in the interfacial layer. As a consequence, the barrier height of a metal–semiconductor system tends to decrease, whereas the barrier height increases for *n*-type devices. The experimental data on barrier height reported by Card[2] can be satisfactorily explained on the basis of the above theoretical model. Recently, the model was extended to a metal–insulator–semiconductor (MIS)-tunnel structure in the presence of a mixed interface comprised of acceptors and donors and interface reaction and the electrical characteristics of the device were studied in detail.[7]

Although the salient features of aging in an $Al-SiO_2-Si$ system were accounted for in terms of a chemical reaction between Al and the SiO_2 layer,[6] it should, however, be mentioned that the features of aging and its subsequent interpretation may not be same for devices having metal contacts other than aluminum. This is because the reactivity of the SiO_2 layer with the adjacent metal is different for different metals and, consequently, the composition of the interface (determined by the reaction product) and the rate at which the composition changes would depend upon the choice of metal. There may be other complexities that arise during processing of the device. For example, in the case of vacuum evaporation of metal onto a silicon substrate with a SiO_2 surface layer, the highly energetic evaporated metal at-

a)Electronic mail: projnan@cubmb.ernet.in

oms release Si atoms from the SiO_2 network by collisions. One cannot possibly rule out further chemical changes when the evaporated atoms strike the SiO_2 layer at elevated temperature. It therefore follows that there is no unique way by which to describe metal–semiconductor interfaces and their aging processes, instead, these interfaces are specific for specific devices and determined by the choice of metal and processing conditions. Because of this, it is necessary for the characteristic features of aging of metal–semiconductor devices be studied in depth with special emphasis on the contact metal used and its interaction with the interface. In this work, a particular metal–semiconductor device, namely, a Ni–*p*-Si contact, was chosen and its aging characteristics are studied. In Sec. II, fabrication and measurement details are presented. The experimental results for the current, conductance, capacitance, and barrier height are discussed in Sec. III. The features of aging observed are explained by developing a theoretical model in Sec. IV. Finally, the important conclusions arrived at are summarized in Sec. V.

II. DEVICE FABRICATION AND ELECTRICAL MEASUREMENTS

A one side polished *p*-type silicon wafer was cleaned sequentially in distilled water, trichloroethylene, acetone, and methanol in an ultrasonic cleaner. Ohmic contact was established by depositing Al on the unpolished surface of the wafer by means of resistive evaporation at 10^{-5} mbar as pressure and subsequent heating *in situ* at 500 °C. Ni contacts of $3.14\times10^{-2}\,\mathrm{cm}^2$ are defined on the polished surface of the wafer by evaporation at the same pressure. The dc measurements were made by an HP E3631A triple output dc power supply and a HP 34401A DMM. The ac measurements such as capacitance and conductance were made with the help of an HP 4263B LCR meter and a SRS 830 DSP lock-in amplifier. The latter was used to specifically study the conductance and capacitance behavior at different frequencies. All measurements were made at different time intervals so as to study the aging characteristics of the device.

Measurements of physical quantities such as the saturation current, the barrier height, and the ideality factor of the device were made using the well known current–voltage ($I-V$) relation described in the thermionic emission model[8] given by

$$I=I_s[\exp(qV/nkT)-1], \tag{1}$$

where I_s is the saturation current of the device given by

$$I_s=A\,A^*T^2\exp(-q\,\phi_{bp}/kT), \tag{2}$$

where A is the area of the device, A^* the Richardson constant, T the temperature, ϕ_{bp} the barrier height of the device, and the other terms have their usual meaning. A plot of the logarithmic current as a function of the bias voltage yields the saturation current and the ideality factor (from the intercept and slope, respectively). Measurement of the diffusion potential was made using the capacitance–voltage ($C-V$) method from reasonably linear $1/C^2$ vs V characteristics.

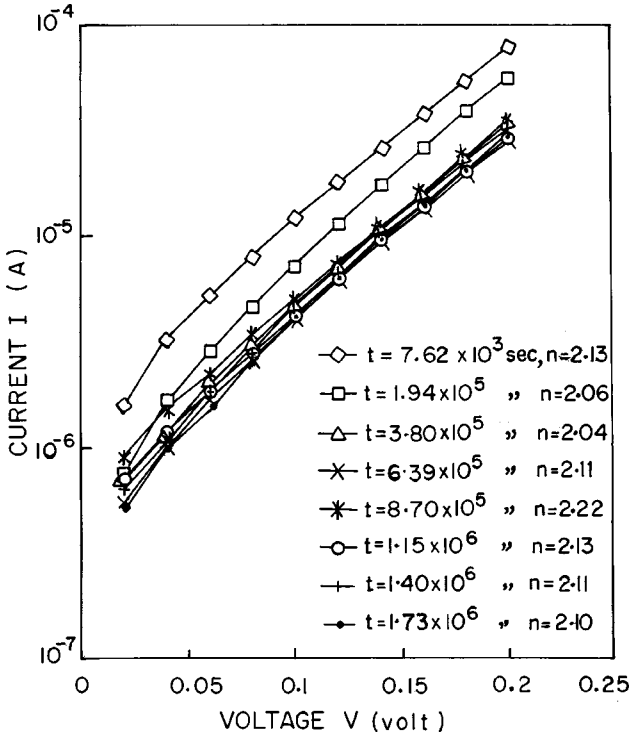

FIG. 1. Current–voltage characteristics of a Ni–*p*-Si contact at different aging times.

III. FEATURES OF AGING

A. The dc characteristics

The dc current–voltage characteristics of the Ni–*p*-Si contact were found to be linear over a certain range of bias voltage limited only by the series resistance of the device at higher bias and exhibit the effect of aging. These characteristics are shown in Fig. 1 for measurements made at different aging times. It is apparent from Fig. 1 that the current decreases gradually as the aging time increases. Interestingly, the change in the current with aging is significant only for the first few measurements. For later measurements, the change becomes insignificant. This feature may be more clearly understood once the variation in device current is examined as a function of the aging time t. Figure 2 illustrates the nature of the variation of the current (at $V=0.2\,\mathrm{V}$) and the saturation current as a function of the aging time. In both the cases, the current was found to saturate at the longer aging times. On the other hand, the ideality factor of the device determined from the linear region of the $I-V$ characteristics seems to be very weakly dependent on the aging time (Fig. 3). The change in current with the aging time also indicates a possible change in the value of the barrier height. When the barrier height is calculated from the saturation current density, an initial increase in barrier height with the aging time has been noticed (Fig. 4). However, the barrier height stabilizes after longer aging.

B. The ac characteristics

The effect of aging was also found to be important for the ac characteristics of the device. Figure 5 shows the conductance–frequency characteristics of the device at dif-

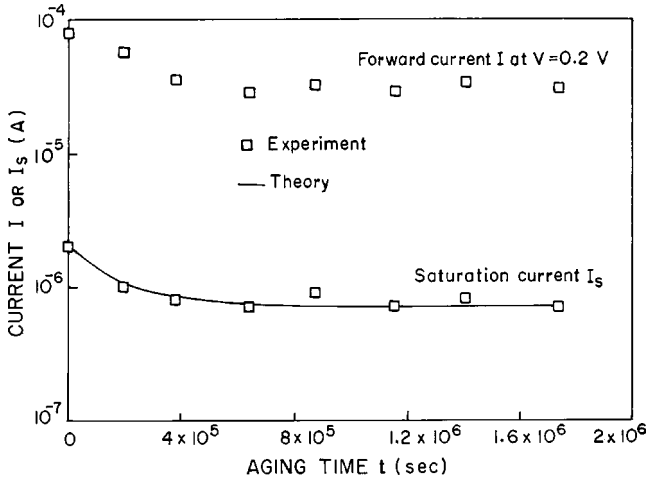

FIG. 2. Variation of current as a function of the aging time in a Ni–*p*-Si contact.

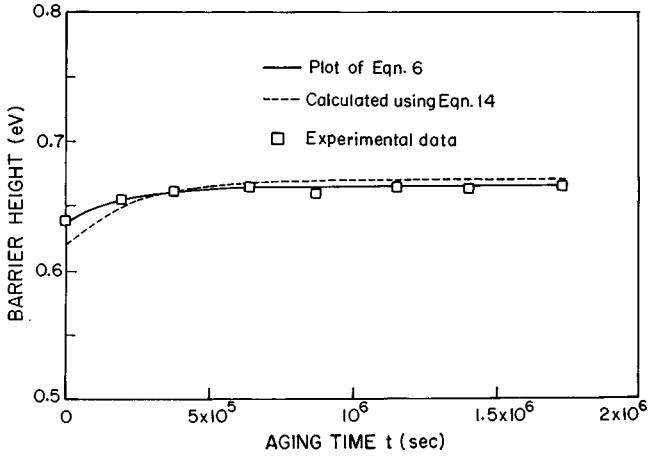

FIG. 4. Variation of the barrier height of a Ni–*p*-Si contact as a function of the aging time.

ferent aging times. These characteristics are in general nonlinear and very sensitive to the aging time. At lower frequencies, the conductance decreases with the aging time at a rate that diminishes as the aging process continues. A similar feature was also noticed in the capacitance–frequency plot (Fig. 6). As can be seen in Fig. 6, the nature of the variation shows a decreasing trend in capacitance with the aging time, but at a much more reduced rate for longer aging when the frequency is low.

The voltage behavior of the high frequency capacitance measured at 100 kHz is shown in Fig. 7 for different aging times. Unlike capacitance–frequency characteristics, the capacitance–voltage plots show a variety of features. The characteristics in general exhibit a rapid decrease in the capacitance as the voltage is varied from the forward to the reverse direction. The effect of aging has been found to be more significant in the forward direction. A large increase in forward capacitance leads to excessive nonlinearity in conventional $1/C^2$ vs V characteristics that prevents estimation of the diffusion potential and doping concentration in most cases. Only characteristics corresponding to aging time $t = 1.59\times10^6$ s (Fig. 8) were found to be reasonably linear over a particular range of voltage that allowed estimation of the doping concentration of about 1.16×10^{15} cm^{-3} and diffusion potential of nearly 0.667 V.

IV. THEORETICAL MODEL AND INTERPRETATION

The features of aging in a Ni–*p*-Si system can best be described by assuming an interfacial SiO_2 layer between the Ni contact and silicon. The changing character of the interface in the present case is somewhat different from in the $Al-SiO_2-Si$ system, where a chemical reaction between the Al and SiO_2 layer results in a net increase in silicon concentration until saturation is established at longer aging time. In the latter system a chemical reaction takes place primarily in the forward direction, yielding atomic silicon in the interfacial region. Being a fourfold electron trap, the atomic silicon yields negative charge density in the interfacial layer and thereby reduces the barrier height in the case of *p*-type devices. If such a mechanism is also valid in the present case, one expects a decrease in the barrier with the aging time similar to in the case of the $Al-SiO_2-p$-Si sys-

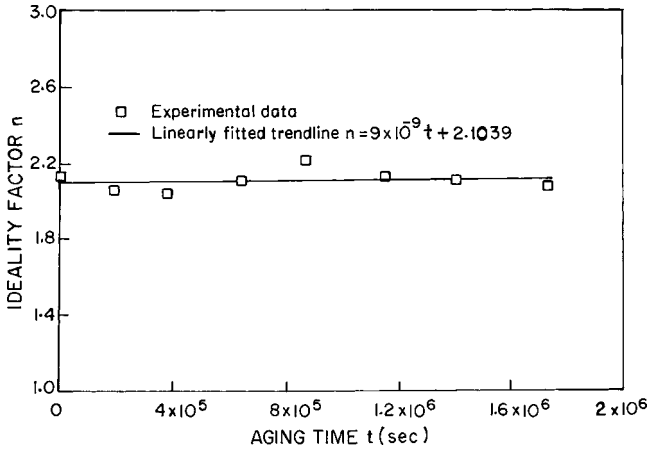

FIG. 3. Variation of the ideality factor of a Ni–*p*-Si contact with the aging time.

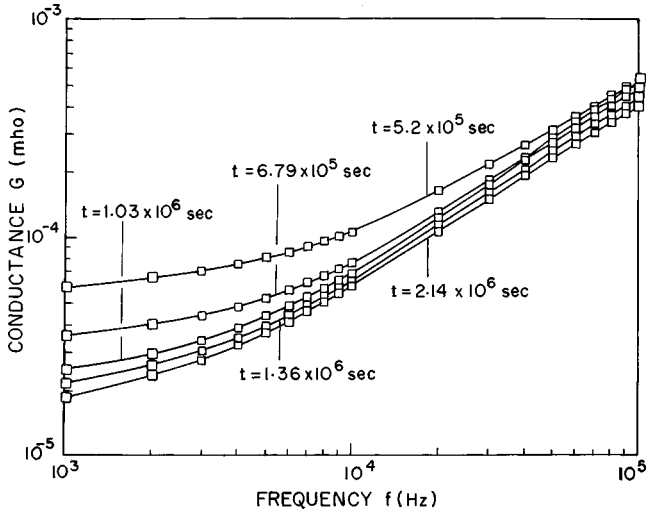

FIG. 5. Conductance–frequency plots of a Ni–*p*-Si contact at different aging times.

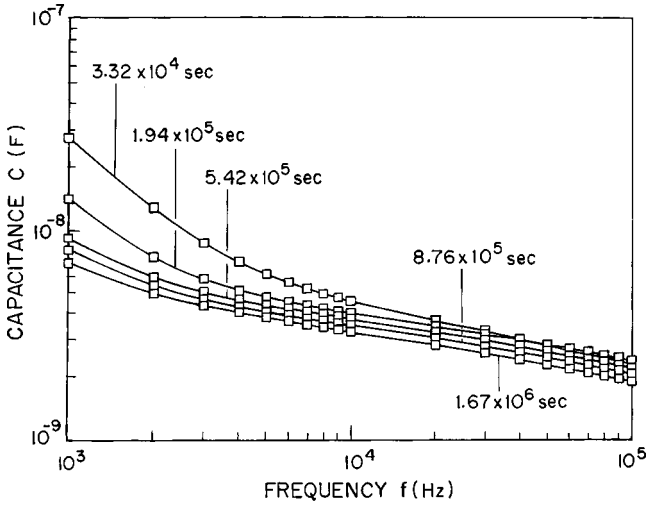

FIG. 6. Capacitance–frequency plots of a Ni–*p*-Si contact at different aging times.

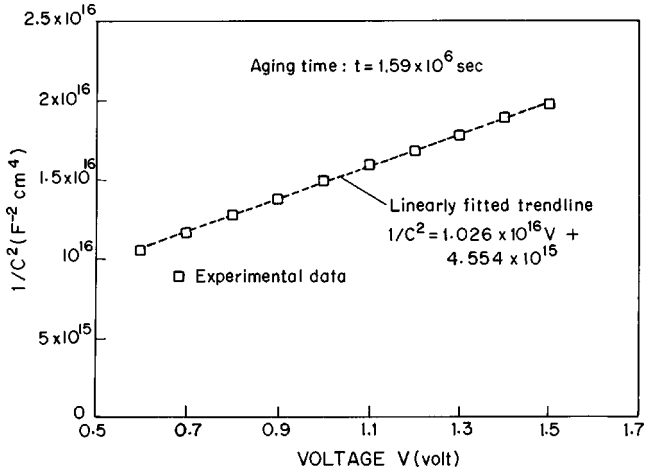

FIG. 8. $1/C^2$ vs V characteristics of a Ni–*p*-Si contact at aging time $t = 1.59\times 10^6$ s.

tem. However, the observed nature of variation of the barrier with the aging time is found to be just the opposite (Fig. 4). To account for this opposite variation, one might look for an alternative explanation such as, that, due to interfacial reaction, a decrease in the interface state density has occurred. But, this seems to be inconsistent with the observed change in the device's ideality factor. Although the ideality factor is not very sensitive to the aging time, the nature of the variation indeed suggests an increase in the density of states, for which the barrier height is expected to decrease. The above inconsistency has prompted reevaluation of the reaction mechanism in MIS systems, specifically in the $Ni-SiO_2-Si$ system. It may be mentioned here that, while depositing metal by means of evaporation, the highly energetic metal atoms may break SiO_2 bonds locally and produce atomic silicon. Again, deposited Ni atoms may react with the SiO_2 layer at a much more elevated temperature (the temperature of the evaporated Ni atoms is assumed to be close to the evaporation temperature) and atomic silicon is liberated.

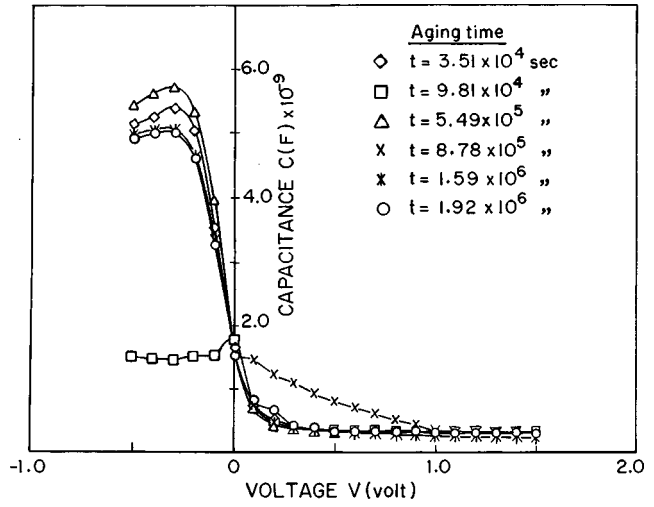

FIG. 7. Capacitance–voltage characteristics of a Ni–*p*-Si contact at different aging times.

Thus, the above two processes whether operating collectively or individually yield atomic silicon and can be considered a generation process. At the same time, a reverse reaction that leads to a decrease in the free silicon concentration can be considered to be a recombination process. Assuming the initial free silicon surface concentration at $t=0$ to be $N_{\mathrm{Si}}(0)$, one can obtain decay in the concentration of Si atoms due to reconversion of free silicon into SiO_2. The rate at which the concentration of silicon atoms changes is

$$dN_{\mathrm{Si}}(t)/dt = -\beta_R N_{\mathrm{Si}}(t), \tag{3}$$

where β_R is the rate constant for the interfacial reaction. The above equation can be integrated as follows:

$$\int_{N_{\mathrm{Si}}(0)}^{N_{\mathrm{Si}}(t)} dN_{\mathrm{Si}}(t)/N_{\mathrm{Si}}(t) = -\beta_R \int_0^t dt, \tag{4}$$

Upon integration Eq. (4) yields

$$N_{\mathrm{Si}}(t) = N_{\mathrm{Si}}(0)\exp(-\beta_R t). \tag{5}$$

The barrier height of the device can be evaluated by including the above decay in the free Si concentration described by Eq. (5) and adopting the procedure discussed in Ref. 6. The mathematical derivation carried in this way resulted in a new expression for barrier height given by

$$\phi_{bp} = \phi_{bp}(0) - C\exp(-\beta_R t), \tag{6}$$

where $C = qN_{\mathrm{Si}}(0)\,\delta C_2/\varepsilon_i$, $C_2 = \varepsilon_i/(\varepsilon_i + q^2\delta D_{it})$, D_{it} is the interface state density, δ the oxide layer thickness, $\phi_{bp}(0)$ the barrier height at $t=0$, and the other terms have their usual meaning. The theoretical barrier height values calculated on the basis of Eq. (6) are plotted in Fig. 4 for comparison with the experimental values of the barrier height. The values of parameters $\phi_{bp}(0)$, C, and β_R that satisfactorily explain the experimental values of the barrier height at different aging times were found to be 0.665 and 0.028 eV and $4.5\times 10^{-6}\,\mathrm{s}^{-1}$, respectively. It should be men-

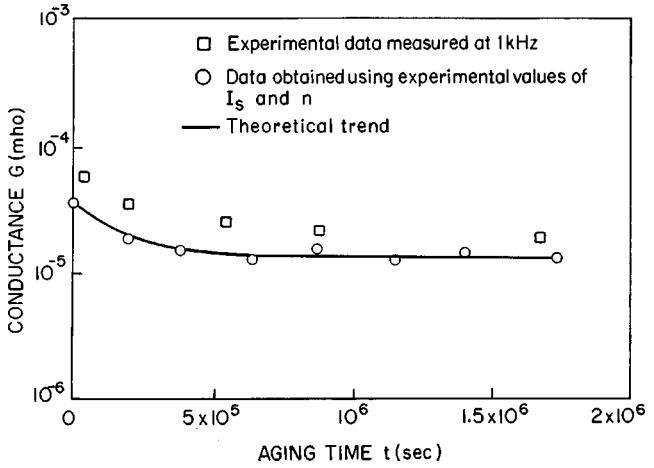

FIG. 9. Variation of low frequency conductance of a Ni–*p*-Si contact with the aging time.

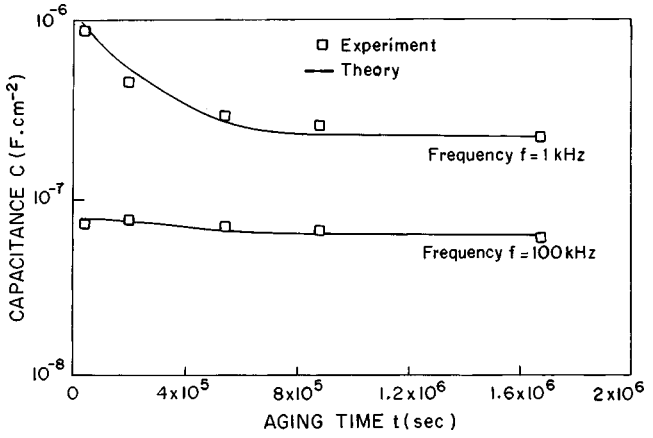

FIG. 10. Variation of low and high frequency capacitance of a Ni–*p*-Si contact as a function of the aging time. The continuous curves represent theoretical plots generated with the help of Eqs. (8)–(14). The interface state densities at frequencies of 1 and 100 kHz are considered to be 7×10^{12} and $3.9\times10^{11}\,\mathrm{cm}^{-2}\,\mathrm{eV}^{-1}$, respectively.

tioned here that the nature of variation of the barrier height in the present case is exactly opposite to that of the $Al-SiO_2-p$-Si system.

The salient features of the conductance–frequency characteristics measured at different aging times can be explained on the basis of modification of the barrier height. For instance, the gradual decrease in value of the conductance with aging signifies a gradual increase in the barrier height. The rate at which the conductance changes is insignificant at longer aging times since the barrier tends to attain a saturation value according to Eq. (6). As a typical example, the conductance values (measured at frequency $f=1$ kHz) at different aging times were considered to examine to what extent the aging behavior can be explained on the basis of a change in barrier height. It should be mentioned here that the conductance values at the above frequency should resemble the dc conductance values since the interface states at this frequency do not contribute appreciably to the total conductance of the device. The dc conductance G can be obtained directly from the $I-V$ relation [Eq. (1)] given by

$$G=dI/dV=qI_s/nkT=qI_s\exp(-qV/nkT)/nkT. \quad (7)$$

At $V=0$, the conductance comes out to be qI_s/nkT. Thus, zero bias dc conductance can be obtained from known values of I_s and n. The conductance values are calculated in two ways. First, the values of I_s and n obtained from the $I-V$ characteristics at different aging times are used in the calculation. These results are plotted in Fig. 9 (open circles). Second, the experimentally fitted relations for I_s and n were used to obtain a theoretical trend. The relation that fits the I_s values is obtained directly using Eqs. (2) and (6), keeping the values of parameters $\phi_{bp}(0)$, C, and β_R the same as those used to explain the experimental barrier height data at different aging times (i.e., 0.665 and 0.028 eV and $4.5\times10^{-6}\,\mathrm{s}^{-1}$, respectively). The relation for the remaining parameter, n, with the aging time is obtained by fitting the measured data given by $n=9\times10^{-9}t+2.1039$ (see Fig. 3). The theoretical trend obtained in this way is shown in Fig. 9 (continuous curve). These conductance values can be compared with the ac conductance values measured at 1 kHz in same figure. It is seen that the theoretical trend explains the general nature of the variation of device conductance. However, the experimental ac values are somewhat larger than the dc values. The excess conductance may be attributable to carrier transport via parasitic shunt resistance.[9]

The capacitance relation of a metal–semiconductor contact is much more involved in the presence of interface states, an interfacial oxide layer, and an interfacial reaction.[7] However, to identify the salient features of aging, a much simpler approach can be adopted based on the assumptions that the drop in voltage across the interfacial layer is small, the interfacial layer capacitance is much larger than the capacitance of a parallel combination of the depletion layer and interface state capacitance, and the interface state conductance is negligible. These assumptions lead to equivalent capacitance that is described by the sum of the depletion layer and parasitic interface state capacitance. Device capacitance in the same form was postulated by Vasudev *et al.*[10] Subsequently, the conditions under which this assumption is valid were discussed.[11] Based on the above description, the effect of aging on the low and high frequency capacitance of the device was analyzed with special emphasis on the interface capacitance that results from charge and discharge processes at interface states. The experimental values of zero bias capacitance at frequencies of 1 and 100 kHz are in particular analyzed by considering interface state capacitance in parallel to depletion layer capacitance. The capacitance of the device in such cases can be written as

$$C=C_{sc}+C_{it}, \quad (8)$$

where C_{it} is the interface state capacitance and C_{sc} is the depletion layer capacitance, expressed as

$$C_{it}=qD_{it}\tan^{-1}\omega\tau/\omega\tau, \quad (9)$$

$$C_{sc}=(q\varepsilon_s N_A/2\psi_s)^{1/2}, \quad (10)$$

where τ is the interface state time constant given by

$$\tau=\exp(q\psi_s/kT)/N_a v_{\mathrm{th}}\sigma, \quad (11)$$

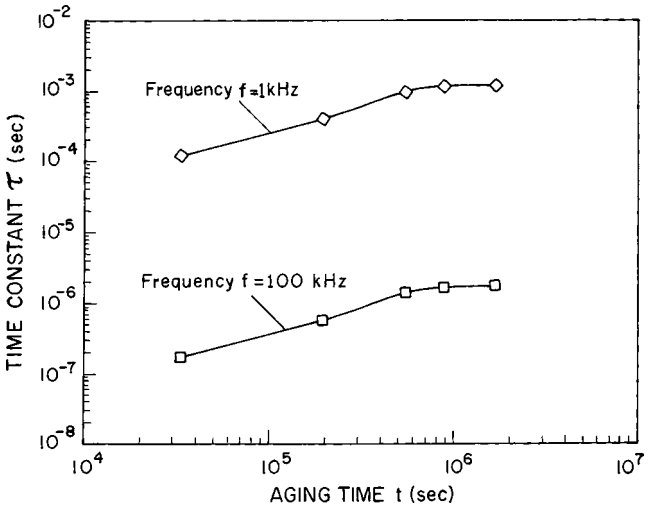

FIG. 11. Plot of low and high frequency time constants of interface states as a function of the aging time. The results were obtained using Eqs. (12) and (13).

where N_a is the doping concentration and the other terms have their usual meaning. It can be seen in Fig. 10 that initially both the low frequency and high frequency capacitance decrease with the aging time until near saturation is established at longer aging time. In both these cases, Eq. (8) satisfactorily explains the nature of variation with two different values of interface state density, namely, $D_{it}=7\times10^{12}$ and $3.9\times10^{11}\,\mathrm{cm}^{-2}\,\mathrm{eV}^{-1}$, respectively, at frequencies of 1 and 100 kHz and time constants given by

$$\tau_{\mathrm{low}}=9.1\times10^{-11}\exp(q\psi_s/kT), \tag{12}$$

$$\tau_{\mathrm{high}}=1.3\times10^{-13}\exp(q\psi_s/kT), \tag{13}$$

where the surface potential is given by

$$\psi_s=0.428-0.07\exp(-4.5\times10^{-6}\,t). \tag{14}$$

The prefactors of Eqs. (12) and (13) yield two values of the capture cross section, namely, $\sigma_{\mathrm{low}}=9.47\times10^{-13}\,\mathrm{cm}^2$ and $\sigma_{\mathrm{high}}=6.63\times10^{-10}\,\mathrm{cm}^2$, respectively, for the low and high frequency cases. The theoretical results obtained with the help of Eqs. (8)–(14) are plotted in Fig. 10 for comparison with the experimental data. Also, the barrier height values obtained using Eq. (14) were plotted in Fig. 4 for comparison with the results obtained from $I-V$ analysis. The variation in time constant for the two states is plotted as a function of the aging time in Fig. 11. It can be seen that the time constants vary linearly with the aging time for the initial measurement but tend to saturate at longer aging times as determined by the surface potential at the contact.

V. CONCLUSION

This study revealed systematic changes in the electrical characteristics of a Ni–*p*-Si contact with the aging time. The dc and ac measurements made on the device have established that these changes follow a specific trend, namely, faster changes for initial measurements followed by much smaller changes at longer aging times. Specifically, the decreases in device current, conductance, and capacitance followed by a tendency of saturation with the aging time are typical features of aging for Ni–*p*-Si contacts. These manifestations reveal enhancement of the barrier height as the aging process continues and can be interpreted in terms of free silicon atoms initially liberated due to the breaking of SiO_2 bonds and/or the interfacial reaction during metal deposition and subsequent exponential decay in their concentration. Interestingly, such exponential decay is in contrast to that in the $Al-SiO_2-p$-Si system where growth of the silicon trap concentration was envisaged. In the present case of the Ni–*p*-Si contact, the exponential law derived explains reasonably well the aging behavior of both the dc and ac properties of the device. In explaining the low and high frequency capacitance values, it was found that at least two different values for the time constant and interface state density are required. Interestingly, the time constants are found to be dependent on the aging time. These observations reveal two varieties of interface states each with different capture cross section and density.

ACKNOWLEDGMENT

This work was carried out under a R&D project sanctioned to the author by the All India Council for Technical Education (AICTE), New Delhi. The author gratefully acknowledges the AICTE for providing funding for the project.

[1] M. J. Turner and E. H. Rhoderick, Solid-State Electron. **11**, 291 (1968).
[2] H. C. Card, IEEE Trans. Electron Devices **ED-23**, 538 (1976).
[3] R. R. Varma, A. McKinley, R. H. Williams, and I. G. Higginbotham, J. Phys. D **10**, L171 (1977).
[4] J. D. Mottram, D. C. Northrop, C. M. Read, and A. Thanailakis, J. Phys. D **12**, 773 (1979).
[5] E. H. Rhoderick and R. H. Williams, *Metal–Semiconductor Contacts*, 2nd ed. (Clarendon, Oxford, 1988), p. 54.
[6] P. Chattopadhyay and K. Das, J. Appl. Phys. **80**, 4229 (1996).
[7] P. Chattopadhyay, J. Appl. Phys. **89**, 364 (2001).
[8] S. M. Sze, *Physics of Semiconductor Devices*, 2nd ed. (Wiley, Singapore, 1999), p. 255.
[9] P. Chattopadhyay, J. Phys. D **29**, 823 (1996).
[10] P. K. Vasudev, B. L. Mattes, E. Pietras, and R. H. Bube, Solid-State Electron. **19**, 557 (1976).
[11] P. Chattopadhyay and B. Raychaudhuri, Solid-State Electron. **36**, 605 (1993).